www.jpeds.com • The Journal of Pediatrics

MKS3-Related Ciliopathy with Features of Autosomal Recessive Polycystic Kidney Disease, Nephronophthisis, and Joubert Syndrome

Meral Gunay-Aygun, MD, Melissa A. Parisi, MD, PhD, Dan Doherty, MD, PhD, Maya Tuchman, Ekaterini Tsilou, MD, David E. Kleiner, MD, PhD, Marjan Huizing, PhD, Baris Turkbey, MD, Peter Choyke, MD, Lisa Guay-Woodford, MD, Theo Heller, MD, Katarzyna Szymanska, Colin A. Johnson, PhD, Ian Glass, MD, and William A. Gahl, MD, PhD

Objectives To describe 3 children with mutations in a Meckel syndrome gene (*MKS3*), with features of autosomal recessive polycystic kidney disease (ARPKD), nephronophthisis, and Joubert syndrome (JS).

Studydesign Biochemical evaluations, magnetic resonance and ultrasound imaging, electroretinograms, IQ testing, and sequence analysis of the *PKHD1* and *MKS3* genes were performed. Functional consequences of the *MKS3* mutations were evaluated by cDNA sequencing and transfection studies with constructs of meckelin, the protein product of *MKS3.*

Results These 3 children with *MKS3* mutations had features typical of ARPKD, that is, enlarged, diffusely microcystic kidneys and early-onset severe hypertension. They also exhibited early-onset chronic anemia, a feature of nephronophthisis, and speech and oculomotor apraxia, suggestive of JS. Magnetic resonance imaging of the brain, originally interpreted as normal, revealed midbrain and cerebellar abnormalities in the spectrum of the "molar tooth sign" that characterizes JS.

Conclusions These findings expand the phenotypes associated with *MKS3* mutations. *MKS3*-related ciliopathies should be considered in patients with an ARPKD-like phenotype, especially in the presence of speech and oculomotor apraxia. In such patients, careful expert evaluation of the brain images can be beneficial because the brain malformations can be subtle. *(J Pediatr 2009;155:386-92)*.

Human ciliopathies, caused by defects in proteins that reside on the cilia or its basal body, include disorders of both the respiratory (motile) and primary (immotile) cilia.[1] Primary cilia are important organelles that sense extracellular chemical and mechanical stimuli such as fluid flow within kidney tubules and bile ducts.

Autosomal recessive polycystic kidney disease (ARPKD) is caused by mutations in *PKHD1*.[2-4] This gene encodes fibrocystin/polyductin,[5,6] a protein that functions in the primary cilia.[7] Affected individuals have fusiform dilatations of the renal collecting ducts, leading to progressive renal insufficiency, and ductal plate malformation of the liver resulting in congenital hepatic fibrosis (CHF) and biliary macrocysts, often referred to as Caroli's syndrome.[8,9] Most patients with ARPKD present perinatally with enlarged, diffusely microcystic kidneys, and approximately 30% die of pulmonary hypoplasia[3,4,10] CHF invariably accompanies ARPKD. Although mild in early childhood, in most patients it eventually leads to portal hypertension (PH), often complicated by esophageal varices and hypersplenism.[11-13] *MKS3* mutations have not been previously associated with ARPKD.

Classic Meckel syndrome (MKS) is a severe, typically perinatally-lethal ciliopathy characterized by cystic dysplastic kidneys and CHF; polydactyly occurs in 55% of affected fetuses, and some patients present with Dandy-Walker malformation or hydrocephalus rather than the classic encephalocele.[14] Five MKS causative genes, *MKS1*, *MKS3, CEP290, RPGRIP1L,* and *CC2D2A,* have been identified.[15-19] The *MKS3* gene, which encodes meckelin, has displayed frameshift, missense, and splice site mutations in several patients with classic MKS who died in the perinatal period with occipital encephalocele, cystic dysplastic kidneys, and postaxial polydactyly.[15] Compared with patients having *MKS1* mutations, those with *MKS3* mutations are less likely to have polydactyly and encephalocele and more likely to have milder central nervous system (CNS) phenotypes with considerable variability.[20-22] Three children with the "molar tooth sign" (MTS) on MRI (a midbrain and cerebellum malformation

ARPKD	Autosomal recessive polycystic kidney disease
CHF	Congenital hepatic fibrosis
CNS	Central nervous system
JSRD	Joubert syndrome and related disorders
MKS	Meckel syndrome
MTS	Molar tooth sign
OMA	Oculomotor apraxia

From the Medical Genetics Branch, National Human Genome Research Institute, Bethesda, MD (M.G.-A., M.T., M.H., W.A.G.); the Intramural Program of the Office of Rare Diseases, Bethesda, MD (M.G.-A., W.A.G.); NEI, Bethesda, MD (E.T); University of Washington, Seattle (M.P., I.G., D.D.); National Institutes of Health Clinical Center, Bethesda, MD (D.K.); Molecular Imaging Program, National Cancer Institute, Bethesda, MD (P.C., B.T.); Laboratory of Pathology, National Cancer Institute, Bethesda, MD (D.E.K.); University of Alabama, Birmingham, AL (L.G.-W.); National Institute of Diabetes and Digestive and Kidney Diseases, Bethesda, MD (T.H.); and Leeds Institute of Molecular Medicine, Leeds, UK (K.S., C.J.)

Supported by the Intramural Research Programs of the National Human Genome Research Institute, National Cancer Institute, National Institute of Diabetes and Digestive and Kidney Diseases, National Eye Institute, and the NIH Clinical Center. The authors declare no conflicts of interest.Registered with www.clinicaltrials.gov (NCT00068224).

 10.1016/j.jpeds.2009.03.045

characteristic of Joubert syndrome and related disorders [JSRD]), displayed mutations in *MKS3*, and 2 fetuses with Meckel-like phenotypes had splice site mutations.[21] Recently, MKS3 mutations have been reported in COACH (cerebellar vermis hypoplasia, oligophrenia, ataxia, coloboma, and hepatic fibrosis) syndrome, a distinct JSRD subgroup with core features of JS plus CHF.[23]

Nephronophthisis is generally characterized by chronic tubulointerstitial nephritis that progresses to renal failure.[24,25] Renal ultrasound shows kidneys of normal or small size with increased echogenicity. In contrast to ARPKD, in which the microscopic cystic dilatations of the collecting ducts appear throughout the cortex and the medulla and result in enlarged kidneys from birth, the renal cysts in nephronophthisis typically localize at the corticomedullary junction and occur after renal failure develops.[24] Blood pressure in juvenile nephronophthisis is typically normal before the onset of renal failure. To date, mutations in 8 different genes (*NPHP1, 3, 4, 5, 6, 7, 8, and 9*) have been identified in juvenile nephronophthisis. *MKS3* mutations have not been associated with NPHP. Approximately 10% to 20% of patients with nephronophthisis have extrarenal organ involvement that resembles other disorders.

In this report, we present detailed findings of 3 children who were ascertained by clinical characteristics of ARPKD and JSRD, but who exhibited pathogenic *MKS3* mutations. These cases illustrate an overlap among ARPKD, nephronophthisis, and JSRD and extend the clinical spectrum of *MKS3*-related ciliopathies.

Methods

The patients and their families were evaluated at the NIH Clinical Center under the intramural protocol number 03-HG-0264 approved by the National Human Genome Research Institute (NHGRI) (www.clinicaltrials.gov, trial NCT00068224). Written informed consent was obtained. Ultrasonographic studies were performed by a single technologist (K.T.D.) using 5- and 7-Mhz transducers (AVI Sequoia Inc, Mountain View, California). For DNA sequencing, all coding exons were amplified from genomic DNA by use of specific intronic primers (primer sequences and conditions are available upon request). Bidirectional sequencing of PCR products was performed using BigDye v3.1 (Applied Biosystems, Foster City, California) terminator chemistry, and reactions were purified with BigDye XTerminator (Applied Biosystems) technology. Extension fragments were separated by capillary electrophoresis on a 3730xl DNA Analyzer (Applied Biosystems). Sequence variants were identified using the software package, Variant Reporter (Applied Biosystems). To test its functional consequences, the C615R mutation was introduced into a pCMV-HA vector, containing the full-length MKS3 wild-type insert, using the QuikChange Site-Directed Mutagenesis Kit (Stratagene Inc, Cedar Creek, Texas) To localize wild-type and mutant meckelin within cells, we transfected 90% confluent IMCD3 cells with 1 μg of plasmid DNA (pCMV-HA-MKS3[wt] and pCMV-HA-MKS3[C615R] constructs) using FuGENE6 transfection reagent(Roche Inc, Basel, Switzerland) After 72 hours of incubation at 37°C/5%CO_2, cells were fixed in ice-cold methanol for 5 minutes and blocked in 1 × PBST, 10% normal goat serum, 1% BSA. Cells were immunostained for the ER marker GRP94 (1:200 rat monoclonal 9G10, Abcam Ltd, Cambridge, United Kingdom), endogenous meckelin (1:100 affinity purified rabbit polyclonal), and the HA epitope (1:100 mouse monoclonal HA-7, Sigma Ltd, St. Louis, Missouri) by standard procedures. Primary antibodies were detected by application of Alexa Fluor fluorescent conjugates (Invitrogen Inc, Carlsbad, California) as follows: goat anti-rat IgG-633, goat anti-rabbit IgG-568 and goat anti-mouse IgG-488, respectively, diluted ×500 in diluent buffer (1×PBST, 1% BSA). DNA was stained with DAPI (2 μg/mL). Confocal images were obtained using a Nikon Eclipse TE2000-E confocal imaging systems, controlled by EZ-C1 3.50 (Nikon Ltd, Tokyo, Japan) software. Z-stacks were taken every 0.5 μm, and cells were assessed for immunostaining in the apical region (within the first 2.5 μm of the cell, above the nucleus) or in the mid-cell regions (below the apical region but above the last 1 μm of the cell). Images were processed in Metamorph, and figures were assembled using Adobe Photoshop CS3 (Adobe Systems Inc, San Jose, California).

Results

Patient 1 (PKD-238) is an 8 year-old boy diagnosed with ARPKD at week 19 of gestation, when routine prenatal ultrasound showed diffusely hyperechoic and enlarged fetal kidneys with loss of corticomedullary differentiation. The amount of amniotic fluid was initially normal but progressively decreased. Fetal growth was normal, and no other anomalies were detected. The patient was delivered vaginally at 36 weeks without complications. Urine output was normal. Serum creatinine peaked at 1.6 mg/dL on the third day of life, decreased to 0.4 mg/dL at 1 month, and remained normal for the first 6 years of life. Severe hypertension, diagnosed on the first day of life, was difficult to manage with 2 antihypertensives, and left ventricular hypertrophy developed. This resolved after 2 years of age, when the hypertension became easier to control. Hyponatremia required oral sodium chloride supplements until 7 months of age. Marked polyuria and polydipsia were present. A normocytic normochromic anemia appeared at 1 month and persisted despite iron supplementation. Liver enzymes and liver ultrasound were unremarkable at birth. By age 5 years, liver enzymes were elevated; ALT and AST ranged between 100 and 250 U/L and AP between 450 and 500 U/L. Synthetic function of the liver remained intact. A liver biopsy at age 7 years showed CHF (**Figure 1**, F). Central hypotonia and motor delays were noted after 6 months. At 12 months, a diagnosis of global developmental delay and speech apraxia prompted an extensive evaluation, which included a normal eye examination. An MRI of the brain performed at 14 months of age was reported as normal, resulting in

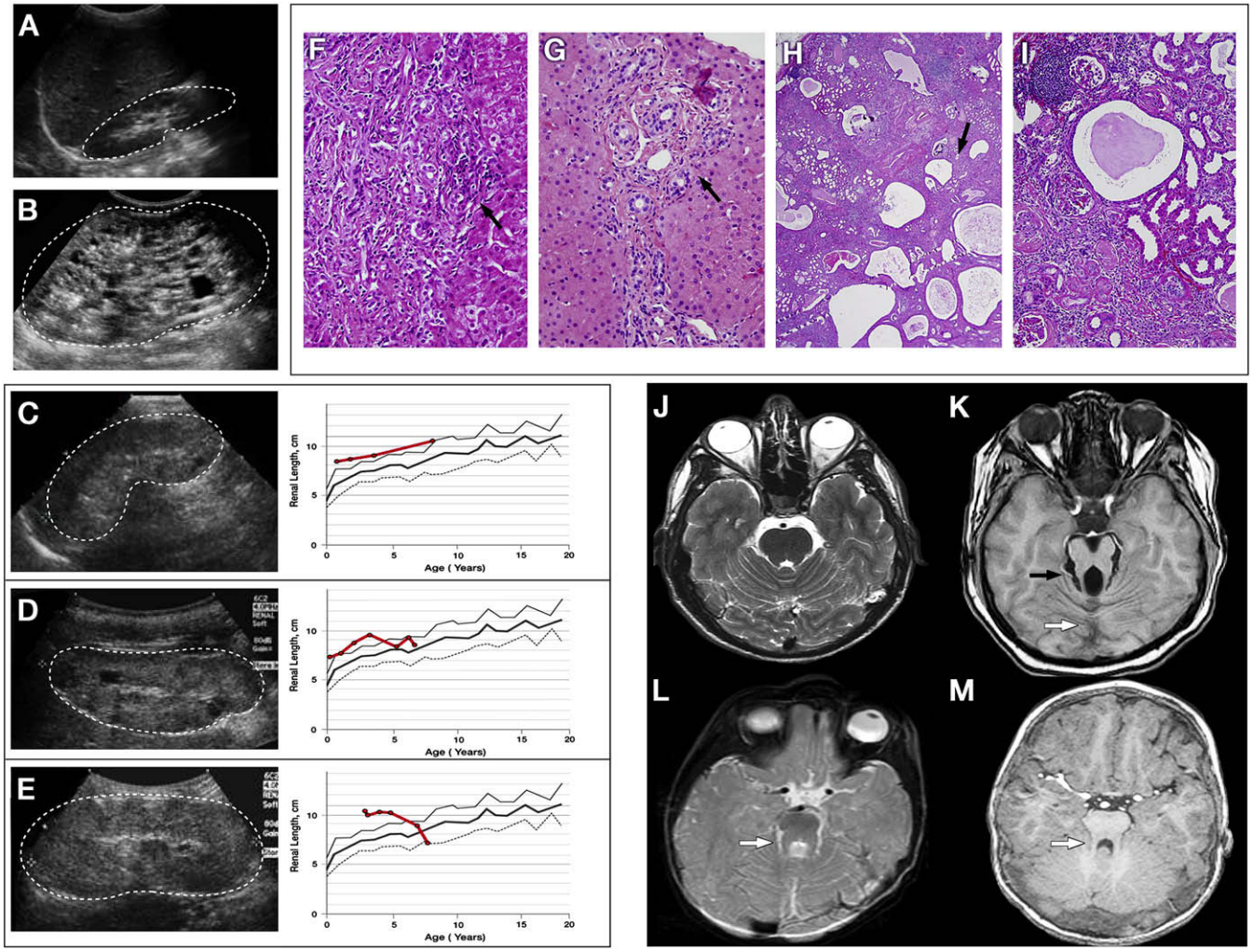

Figure 1. Summary of kidney, liver, and brain findings of patients 1 through 3. Ultrasound image shows normal kidney **A**, measuring 8 cm at 5 years of age, in comparison with the kidney of a typical patient with ARPKD **B**, measuring 14 cm at age 5 years. Patients' kidney ultrasound findings (dots outline the kidneys) (left panel of **C** through **E**) and kidney growth over the years are shown (average of right and left), measured on ultrasound and plotted against age (right panel of **C** through **E**). Bold solid red line indicates the patients' kidney length for age, with the normal mean indicated by a bold gray line, +2 SD by a solid gray line and −2 SD by a dotted gray line. Kidneys of patient 1 **C**, remained large (10.3 cm) at 8 years of age. Kidneys of patient 2 measured 9.2 cm at age 2 years 10 months **D**, continued above 2 SD until approximately 4 years of age, and then declined toward normal size as she progressed into end-stage renal failure. Kidneys of patient 3 measured 11.1 cm at age 4 years, 2 months **E**, remained large at approximately 4 SD until 5 years of age, and declined sharply in size as he progressed into end-stage renal disease. All 3 patients (**C** through **E**) exhibited enlarged, diffusely hyperechoic kidneys with loss of corticomedullary differentiation and a few scattered macrocysts (arrow) indistinguishable from ARPKD kidneys **(B)**. The liver biopsies of patient 1 **F** and patient 2 **G** show congenital hepatic fibrosis characterized by expanded portal areas with persistence of embryonic bile duct structures (arrows). The extracted kidney of patient 3 at low **H** and high **I** magnification shows cysts scattered throughout the cortex and medulla and accumulating at the corticomedullary junction (arrow, **H**). Lymphoid aggregates with chronic interstitial nephritis, glomerulosclerosis, and tubular atrophy (**H** and **I**) are shown. Normal brain MRI on axial cut through the superior cerebellar peduncles **J** is shown. The "molar tooth sign" seen in JSRD **K** caused by the combination of a hypoplastic cerebellar vermis (white arrow), elongated and thickened superior cerebellar peduncles (black arrow), and abnormally deep interpeduncular fossa is shown. The brain MRI of patient 1 **L**, initially reported as normal, in fact shows a subtle molar tooth sign (white arrow). The brain MRI of patient 3, **M** initially reported as normal, shows slightly elongated and pointed superior cerebellar peduncles (white arrow) with hypoplastic and dysplastic vermis on retrospective reevaluation.

persistence of the diagnosis of ARPKD, with probable cerebral palsy. Head size, weight, and height remained at the 50th percentile.

On evaluation at the NIH Clinical Center at age 8 years, ultrasound revealed enlarged hyperechoic kidneys with small macrocysts in the cortex and medulla (Figure 1, C). Other

Table I. Laboratory findings at NIH evaluation

	Normal Range	Patient 1	Patient 2	Patient 3
Age at evalution (Y)/sex	–	8/M	6.5/F	10/M
Hb (g/dL)	11.5–15.5	11.3*	10.5*	11.2*
Htc (%)	35–45	33.2*	31.7*	34.5*
MCV (fL)	77–95	80.2	87	79.9
Serum creatinine (mg/dL)	0.25–0.65	1.3*	1.64*	Posttransplant
Serum cystatin C (mg/L)	0.55–1.03	2*	2.06*	Posttransplant
Creatinine clearance (mL/min/1.73 m^2)	90–170	40*	25*	Posttransplant
ALT (U/L)	6–41	135*	413*	66*
AST (U/L)	9–34	158*	290*	61*
AP (U/L)	37–520	383	651*	376
GGT (U/L)	7–38	179*	355*	105*
Prothrombin time (s)	13.2–14.6	13.6	13.1	14.3
Albumin (g/dL)	3.7–4.7	4	3.9	4.1

Hb, hemoglobin; Hto, hematocrit; MCV, mean corpuscular volume; ALT, alanine amino transferase; AST, aspartate amino transferase; AP, alkaline phosphatase.
*Abnormal values.

laboratory findings are presented in Table I. The liver was diffusely hyperechoic and inhomogeneous on ultrasound, without cysts. The spleen was mildly enlarged at 11.5 cm. Ophthalmologic examination showed mild, slow torsional nystagmus when fixating clockwise. The retina, optic nerve, and anterior chamber were normal. Snellen visual acuity was 20/50 OD and 20/40 OS. On the Wechsler Intelligence Scale for Children-Fourth Edition (WISC-IV), the verbal comprehension index was 63 (1st percentile). His perceptual reasoning index was 61 (1st centile). A full-scale IQ could not be derived because he did not complete the test. Sequencing of the *PKHD1* gene revealed no pathogenic variations. Given the milder CNS phenotype and frequent absence of polydactyly in reported patients with *MKS3* mutations, we sequenced the *MKS3* gene. The boy was compound heterozygous for a novel splice site mutation in exon 2, c.224-2 A>T, and a missense mutation in exon 18, c.1843 T>C, resulting in amino acid substitution p.Cys615Arg. Segregation analysis showed that the c.224-2 A>T splice site mutation was inherited maternally and the Cys615Arg missense mutation was inherited paternally. Retrospective evaluation of his brain MRI obtained at 14 months of age, initially interpreted as normal, demonstrated features of MTS (Figure 1, L).

Patient 2 (PKD-271) is a 6.5 year-old girl with large hyperechoic kidneys with scattered cysts on prenatal ultrasound. There was no oligohydramnios and the pregnancy, delivery, and neonatal course were uncomplicated. Postnatal ultrasound confirmed the prenatal findings. At age 1 week, she had hypertension that was difficult to control, resulting in transient left ventricular hypertrophy despite 2 antihypertensive medications. Renal function was normal. At 4 months of age, a neuro-ophthalmological evaluation, prompted by the history of oculomotor apraxia (OMA) in her older brother (patient 3), revealed OMA and mild generalized hypotonia. She has had chronic normochromic normocytic anemia since early infancy and remained on iron supplementation with minimal response. There was polyuria and polydipsia. Her growth was normal. She developed chronic elevation of liver enzymes (ALT and AST >200 U/L and AP >400 U/L) and splenomegaly. At the NIH evaluation, her glomerular function was impaired, normochromic normocytic anemia persisted, and liver enzymes were elevated (Table I). Synthetic function of the liver was intact. Eye examination was normal except for slight slowing of saccades. Snellen visual acuity was 20/25 OD and 20/32 OS. ERG was normal. Cognitive evaluation showed slight articulation problems, but she was 100% comprehensible. On the WISC-IV, she obtained a full-scale IQ of 95 (37th percentile; average range) with variable index scores; verbal comprehension, working memory, perceptual reasoning, and processing speed were 99, 102, 98, and 83, respectively.

Patient 3 (PKD-272) is the 10 year-old brother of patient 2. He was born at term after a normal pregnancy. The delivery and neonatal period were uneventful. At 12 months he was diagnosed with oculomotor apraxia associated with central hypotonia and mild developmental delay. He made progress with speech and physical therapy. At age 3, a screening ultrasound, prompted by the diagnosis of polycystic kidney disease in his younger sister (patient 2), showed enlarged hyperechoic kidneys; at the same visit, hypertension was diagnosed. Two antihypertensive medications achieved borderline blood pressure control. Renal function was normal. A brain MRI performed at age 22 months was interpreted as normal. He began to have decline in glomerular function at age 5.5 and underwent kidney transplantation at age 8 years. The extracted native kidneys exhibited moderate chronic interstitial nephritis, glomerulosclerosis, tubular atrophy, and nephrocalcinosis as well as cysts, mostly accumulated at the corticomedullary junction but also scattered throughout the cortex and medulla (Figure 1, H and I). He had polyuria and polydipsia and chronic normochromic normocytic anemia since early infancy. His growth was normal. He developed chronic elevation of liver enzymes and splenomegaly and had an episode of cholangitis at age 5 years. A liver biopsy performed at 5.5 years showed CHF (Figure 1, G). Eye evaluation at NIH revealed slight slowing of the saccades, without significant evidence of OMA. His vision was 20/20 OU. The optic discs and retina were normal. On ERG, mixed responses were slightly subnormal but cone responses were normal. The full-scale IQ of patient 3 was 76, with index scores of 81, 71, 94, and 75, respectively.

Sequencing of *PKHD1* in patients 2 and 3 was negative. Similarly, testing for the common *NPHP1* gene deletion and for *NPHP2* mutations was negative. Sequencing of the *MKS3* gene showed that both siblings were homozygous and their parents were heterozygous for the missense mutation c.1843 T>C, p.Cys615Arg in exon 18 (Figure 2, B). On retrospective review, subtle findings within the spectrum of the MTS were noted on patient 3's brain MRI performed at 22 months (Figure 1, M).

To document the consequences of the splice mutation, we amplified and sequenced the RT PCR product of RNA extracted from the transformed peripheral blood lymphocytes of patient 1 and demonstrated that the c.224-2 A>T mutation resulted in skipping of exon 2 (Figure 3, A and B; available at www.jpeds.com) with a subsequent frameshift

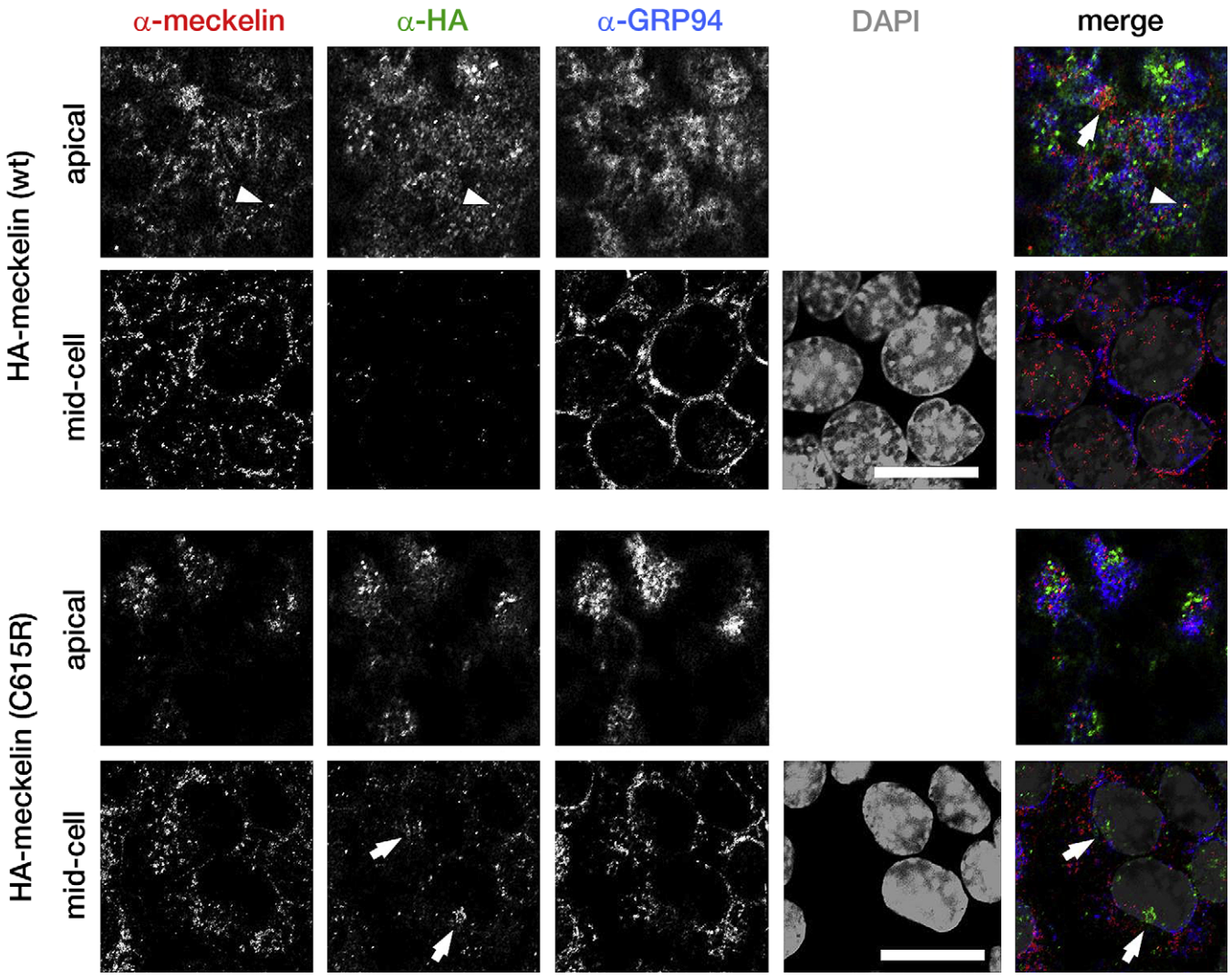

Figure 2. Immunofluorescent confocal microscopy of the polarized, ciliated IMCD3 cell-line, after transfection with an HA-epitope tagged construct of meckelin with the p.C615R mutation, compared with wild-type. Top panels: Immunostaining of endogenous meckelin (red), transfected wild-type HA-tagged meckelin (green), endogenous GRP94 (a marker of the endoplasmic reticulum; blue), and DAPI (grey). z-Stacks were taken every 0.5 μm and cells were assessed for immunostaining in the apical region (within the first 2.5 μm of the cell, above the nucleus) or in the mid-cell regions (below the apical region, but above the last 1 μm of the cell). The igures show individual z-stacks from the apical and mid-cell regions, as indicated. Endogenous meckelin colocalized with wild-type HA-tagged meckelin at both cilia (arrowheads) and at the apical cell surface (arrow). Wild-type HA-tagged meckelin is absent from mid-cell subcellular locations. Note that endogenous meckelin colocalizes with some components of the endoplasmic reticulum. Bottom panels: Immunostaining as above, but transfected with HA-tagged meckelin containing the p.C615R mutation. Mutant meckelin does not appear to extensively colocalize with endogenous meckelin at the apical cell surface and is aggregated in the mid-cell region (arrows). Scale bars = 5 μm.

in exon 3, resulting in premature truncation after 79 amino acids. To assess subcellular localization of wild-type and mutant (p.Cys615Arg) meckelin, we used immunofluorescent confocal microscopy of the polarized, ciliated IMCD3 cell-line. Both endogenous and transfected wild-type HA epitope-tagged meckelin are folded in the ER and transported efficiently to the apical cell surface and primary cilia (Figure 2, top panel). Very little of the wild-type protein is found at mid-cell z-slices in the confocal images. However, the HA-tagged meckelin containing the C615R mutation is partially retained at the mid-cell regions (Figure 2, bottom panel), possibly in lysosomes, although it can also be transported to the apical cell surface. There was no colocalization of this mutant protein with primary cilia (data not shown).

Discussion

These 3 children with *MKS3* mutations are unique in that they represent an overlap among ARPKD, nephronophthisis,

and JSRD (Table II). They share the following clinical features: (1) enlarged kidneys with diffuse microcystic changes (Figure 1, C through E) resulting in progressive renal failure in childhood (ARPKD); (2) early-onset severe hypertension (ARPKD); (3) chronic normocytic normochromic anemia (nephronophthisis); (4) urinary concentration defect resulting in polyuria and polydipsia (ARPKD and nephronophthisis); (5) congenital hepatic fibrosis and portal hypertension (ARPKD and a subset of nephronophthisis); (6) OMA and speech apraxia associated with mild midbrain and cerebellum abnormalities within the spectrum of the MTS (JSRD) (Figure 1, L and M). Features typical of ARPKD include increased kidney size with preserved reniform contours reflecting diffuse microcystic changes of the medulla extending to the cortex (Figure 1, B through E) and the presence of severe hypertension beginning years before the decline in glomerular function. Transient neonatal hyponatremia, as seen in patient 1, is another feature typical of ARPKD. However, the presence of CNS abnormalities conflicts with the diagnosis of ARPKD, in which the pathology is limited to the kidneys and the liver. Furthermore, chronic anemia is a classic feature of nephronophthisis, which does not manifest early-onset hypertension before end-stage renal disease and is typically associated with small or normal-sized kidneys (Table II).

Thus, our patients' clinical findings constitute an overlap phenotype among ARPKD, nephronophthisis, and JSRD. The native kidney extracted from patient 3 had features of both ARPKD and nephronophthisis, that is, cysts distributed throughout the cortex and medulla of the kidney (Figure 1, H), moderate chronic interstitial nephritis, marked glomerulosclerosis, and tubular atrophy (Figure 1, H and I). In addition, the CNS abnormalities in these patients, specifically the speech apraxia in patient 1, the OMA in patients 2 and 3, and the MTS in patients 1 and 3 (Figure 1, L and M) are features of JSRD, which can be associated with nephronophthisis and/or CHF. We note that the wpk rat, homozygous for an *MKS3* mutation, was proposed as a model for ARPKD before the identification of its CNS abnormalities.[26] Our patients with *MKS3* mutations appear to recapitulate aspects of that phenotype. Of note, the brain MRIs of patients 1 and 3 were performed and initially interpreted as "normal," apparently because of the subtlety of the findings. An *MKS3*-related ciliopathy should be considered in patients carrying the diagnosis of "ARPKD," especially in the presence of speech apraxia or OMA. In such patients, careful evaluation of brain MRI scans by those with expertise in identifying this specific spectrum of brain abnormalities may be beneficial.

Neither of the 2 *MKS3* mutations we identified in these patients is previously reported. However, both mutations are likely to be pathogenic because of the following data. The cysteine at position 615 of meckelin (the protein encoded by *MKS3*) is completely conserved among human, chimp, dog, mouse, and rat. We did not detect the c.1843 T>C, p.Cys615Arg mutation in 210 control chromosomes. The splice mutation c.224-2 A>T disrupts the universal AG splice acceptor site. Finally, the p.Cys615Arg mutation alters the subcellular localization of meckelin (Figure 2). Meckelin is a ciliary protein associated with an extremely wide phenotypic spectrum, ranging from perinatally lethal Meckel syndrome to an ARPKD/nephronophthisis/JSRD-like phenotype. The p.Cys615Arg mutation is the first *MKS3* mutation described that localizes to the intracellular loop of the meckelin protein (Figure 3, C); *MKS3* mutations associated with MKS primarily localize to the extracellular domain, and mutations in JSRD patients are seen in the extracellular, transmembrane, and intracellular carboxy terminal domains. As more *MKS3* mutations are identified and more ciliopathy patients are screened for defects in multiple ciliary proteins, we may discover the degree to which the clinical variability in *MKS3*-related ciliopathies is explained by the severity and location of the *MKS3* mutations, in contrast to the contribution of modifier genes. One such example of the probable effect of strong modifiers was apparent in an MKS family with 5 affected fetuses displaying a wide variability of central nervous system involvement ranging from severe enchephalocele to completely normal, despite the fact that all 5 fetuses carried the same 2 *MKS3* mutations.[22] This variability suggests that other genes influence the phenotype. ■

Table II. Patients findings compared with features of various ciliopathies

	patient 1	patient 2	patient 3	ARPKD	MKS	JSRD	Juvenile NPHP
Molor tooth sign	+	+	+	-	±	+	±
Enlarged diffusely cystic kidneys	+	+	+	+	+	−	−
Early onset severe hypertension	+	+	+	+	NA*	−	−
Anemia	+	+	+	−	NA*	±	+
Congenital hepatic fibrosis	+	+	+	+	+	±	±

*Unknown because patients with typical MKS do not survive beyond the perinatal period.

We thank the patients and their families, who generously participated in this investigation. We also thank Linda Lukose, MD, Joy C. Bryant, RN, Gretchen Golas, NP, Heidi Dorward, Carla Ciccone, MS, and Kailash T. Daryanani for their assistance.

Submitted for publication Nov 25, 2008; last revision received Jan 20, 2009; accepted March 20, 2009.

Reprint requests: Dr Meral Gunay-Aygun, NHGRI, NIH, 10 Center Drive, Building 10, Room 10C103A, Bethesda, MD 20892. E-mail: mgaygun@mail.nih.gov.

References

1. Fliegauf M, Benzing T, Omran H. When cilia go bad: cilia defects and ciliopathies. Nat Rev Mol Cell Biol 2007;8:880-93.
2. Gunay-Aygun M, Avner ED, Bacallao RL, Choyke PL, Flynn JT, Germino GG, et al. Autosomal recessive polycystic kidney disease and congenital hepatic fibrosis: summary statement of a first National Institutes of Health/Office of Rare Diseases conference. J Pediatr 2006;149:159-64.
3. Guay-Woodford LM, Desmond RA. Autosomal recessive polycystic kidney disease: the clinical experience in North America. Pediatrics 2003;111(5 Pt 1):1072-80.

4. Zerres K, Rudnik-Schoneborn S, Deget F, Holtkamp U, Brodehl J, Geisert J, et al. Autosomal recessive polycystic kidney disease in 115 children: clinical presentation, course and influence of gender. Arbeitsgemeinschaft fur Padiatrische, Nephrologie. Acta Paediatr 1996;85:437-45.
5. Onuchic LF, Furu L, Nagasawa Y, Hou X, Eggermann T, Ren Z, et al. PKHD1, the polycystic kidney and hepatic disease 1 gene, encodes a novel large protein containing multiple immunoglobulin-like plexin-transcription-factor domains and parallel beta-helix 1 repeats. Am J Hum Genet 2002;70:1305-17.
6. Ward CJ, Hogan MC, Rossetti S, Walker D, Sneddon T, Wang X, et al. The gene mutated in autosomal recessive polycystic kidney disease encodes a large, receptor-like protein. Nat Genet 2002;30:259-69.
7. Ward CJ, Yuan D, Masyuk TV, Wang X, Punyashthiti R, Whelan S, et al. Cellular and subcellular localization of the ARPKD protein: fibrocystin is expressed on primary cilia. Hum Mol Genet 2003;12:2703-10.
8. Desmet VJ. Congenital diseases of intrahepatic bile ducts: variations on the theme "ductal plate malformation." Hepatology 1992;16:1069-83.
9. Jorgensen MJ. The ductal plate malformation. Acta Pathol Microbiol Scand Suppl 1977;1-87.
10. Capisonda R, Phan V, Traubuci J, Daneman A, Balfe JW, Guay-Woodford LM. Autosomal recessive polycystic kidney disease: outcomes from a single-center experience. Pediatr Nephrol 2003;18:119-26.
11. Kerr DN, Okonkwo S, Choa RG. Congenital hepatic fibrosis: the long-term prognosis. Gut 1978;19:514-20.
12. Goilav B, Norton KI, Satlin LM, Guay-Woodford L, Chen F, Magid MS, et al. Predominant extrahepatic biliary disease in autosomal recessive polycystic kidney disease: a new association. Pediatr Transplant 2006; 10:294-8.
13. Shneider BL, Magid MS. Liver disease in autosomal recessive polycystic kidney disease. Pediatr Transplant 2005;9:634-9.
14. Fraser FC, Lytwyn A. Spectrum of anomalies in the Meckel syndrome, or: "Maybe there is a malformation syndrome with at least one constant anomaly. Am J Med Genet 1981;9:67-73.
15. Smith UM, Consugar M, Tee LJ, McKee BM, Maina EN, Whelan S, et al. The transmembrane protein meckelin (MKS3) is mutated in Meckel-Gruber syndrome and the wpk rat. Nat Genet 2006;38:191-6.
16. Kyttala M, Tallila J, Salonen R, Kopra O, Kohlschmidt N, Paavola-Sakki P, et al. MKS1, encoding a component of the flagellar apparatus basal body proteome, is mutated in Meckel syndrome. Nat Genet 2006;38:155-7.
17. Baala L, Audollent S, Martinovic J, Ozilou C, Babron MC, Sivanandamoorthy S, et al. Pleiotropic effects of CEP290 (NPHP6) mutations extend to Meckel syndrome. Am J Hum Genet 2007;81:170-9.
18. Delous M, Baala L, Salomon R, Laclef C, Vierkotten J, Tory K, et al. The ciliary gene RPGRIP1L is mutated in cerebello-oculo-renal syndrome (Joubert syndrome type B) and Meckel syndrome. Nat Genet 2007;39: 875-81.
19. Tallila J, Jakkula E, Peltonen L, Salonen R, Kestila M. Identification of CC2D2A as a Meckel syndrome gene adds an important piece to the ciliopathy puzzle. Am J Hum Genet 2008;82:1361-7.
20. Khaddour R, Smith U, Baala L, Martinovic J, Clavering D, Shaffiq R, et al. Spectrum of MKS1 and MKS3 mutations in Meckel syndrome: a genotype-phenotype correlation. Mutation in brief #960. Online. Hum Mutat 2007;28:523-4.
21. Baala L, Romano S, Khaddour R, Saunier S, Smith UM, Audollent S, et al. The Meckel-Gruber syndrome gene, MKS3, is mutated in Joubert syndrome. Am J Hum Genet 2007;80:186-94.
22. Consugar MB, Kubly VJ, Lager DJ, Hommerding CJ, Wong WC, Bakker E, et al. Molecular diagnostics of Meckel-Gruber syndrome highlights phenotypic differences between MKS1 and MKS3. Hum Genet 2007;121:591-9.
23. Brancati F, Iannicelli M, Travaglini L, Mazzotta A, Bertini E, Boltshauser E, et al. MKS3/TMEM67 mutations are a major cause of COACH Syndrome, a Joubert syndrome related disorder with liver involvement. Hum Mutat 2008;30:E432-42.
24. Hildebrandt F, Zhou W. Nephronophthisis-associated ciliopathies. J Am Soc Nephrol 2007;18:1855-71.
25. Salomon R, Saunier S, Niaudet P. Nephronophthisis. Pediatr Nephrol 2008. Jul 18 [Epub ahead of print].
26. Gattone VH 2nd, Tourkow BA, Trambaugh CM, Yu AC, Whelan S, Phillips CL, et al. Development of multiorgan pathology in the wpk rat model of polycystic kidney disease. Anat Rec A Discov Mol Cell Evol Biol 2004;277:384-95.

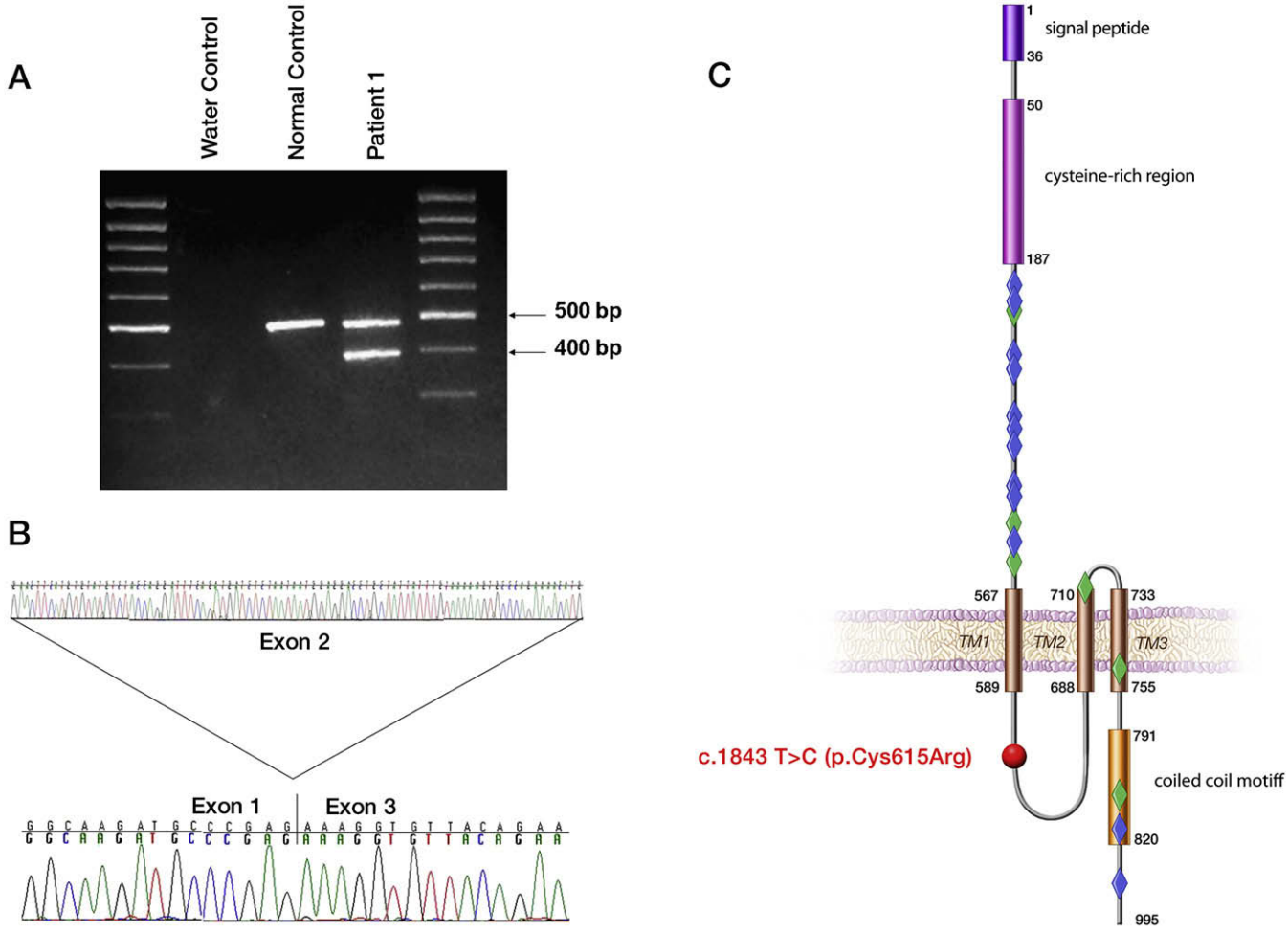

Figure 3. *MKS3* mutations found in patients 1 through 3. Analysis of the c.224-2 A>T splice site mutation at the RNA level (**A** and **B**) is shown. Expected wild-type size (483 bp) is seen in the control, whereas in patient 1 the smaller band (394 bp) corresponds to the transcript lacking exon 2, **A**. Direct sequencing of the RT-PCR product from patient 1 shows skipping from exon 1 to exon 3, **B**. Localization of the p.Cys615Arg mutation (red sphere) to the intracellular loop of the meckelin protein, **C**, in comparison with the location of the mutations reported in MKS (blue diamonds) and JSRD patients (green diamonds) is shown. Modified from Khaddour et al[20].